Journal of Neuroinflammation

RESEARCH

Open Access

iPLA2β loss leads to age-related cognitive decline and neuroinflammation by disrupting neuronal mitophagy

Li Jiao[1], Wenxin Shao[1], Wenqi Quan[1], Longjiang Xu[1], Penghui Liu[1], Jinling Yang[1] and Xiaozhong Peng[1,2,3*]

Abstract

Background During brain aging, disturbances in neuronal phospholipid metabolism result in impaired cognitive function and dysregulation of neurological processes. Mutations in iPLA2β are associated with neurodegenerative conditions that significantly impact brain phospholipids. iPLA2β deficiency exacerbates mitochondrial dysfunction and abnormal mitochondrial accumulation. We hypothesized that iPLA2β contributes to age-related cognitive decline by disrupting neuronal mitophagy.

Methodology We used aged wild-type (WT) mice and iPLA2β$^{-/-}$ mice as natural aging models to assess cognitive performance, iPLA2β expression in the cortex, levels of chemokines and inflammatory cytokines, and mitochondrial dysfunction, with a specific focus on mitophagy and the mitochondrial phospholipid profile. To further elucidate the role of iPLA2β, we employed adeno-associated virus (AAV)-mediated iPLA2β overexpression in aged mice and re-evaluated these parameters.

Results Our findings revealed a significant reduction in iPLA2β levels in the prefrontal cortex of aged brains. Notably, iPLA2β-deficient mice exhibited impaired learning and memory. Loss of iPLA2β in the PFC of aged mice led to increased levels of chemokines and inflammatory cytokines. This damage was associated with altered mitochondrial morphology, reduced ATP levels due to dysregulation of the parkin-independent mitophagy pathway, and changes in the mitochondrial phospholipid profile. AAV-mediated overexpression of iPLA2β alleviated age-related parkin-independent mitophagy pathway dysregulation in primary neurons and the PFC of aged mice, reduced inflammation, and improved cognitive function.

Conclusions Our study suggests that age-related iPLA2β loss in the PFC leads to cognitive decline through the disruption of mitophagy. These findings highlight the potential of targeting iPLA2β to ameliorate age-related neurocognitive disorders.

*Correspondence:
Xiaozhong Peng
pengxiaozhong@pumc.edu.cn
[1]National Kunming High-Level Biosafety Primate Research Center, Institute of Medical Biology, Chinese Academy of Medical Sciences & Peking Union Medical College, 935 Jiaoling Road, Kunming 650118, Yunnan, China
[2]State Key Laboratory of Respiratory Health and Multimorbidity, Innovation for Animal Model, Institute of Laboratory Animal Sciences, National Center of Technology, CAMS & PUMC, Beijing 100021, China
[3]Department of Molecular Biology and Biochemistry, Institute of Basic Medical Sciences, Medical Primate Research Center, Neuroscience Center, CAMS & PUMC, Beijing 100005, China

Introduction

Aging is a complex physiological process characterized by a progressive decline in organismal and cellular structures and functions [1]. The brain is one of the major organs affected by aging, accompanied by the development of neurodegenerative diseases, such as Alzheimer's disease [2] and Parkinson's disease [3]. Many factors can trigger brain aging, including infection, injury, stress, inflammation, malnutrition, and metabolic disorders [4]. During brain aging, the number and function of neurons gradually decrease [5], leading to impaired cognitive function and dysregulation of neurological processes [6]. The prefrontal cortex (PFC) is a critical region in the anterior part of the frontal lobe, responsible for supporting higher cognitive functions, such as working memory. As aging progresses, the PFC is one of the first areas to be affected by brain shrinkage [7] and is also where cognitive abilities tend to decline the earliest. This region is particularly sensitive to stress, normal aging, and age-related diseases such as Alzheimer's disease (AD) [8]. Consequently, the PFC is prone to functional decline during normal aging, particularly during cognitive processes. However, the molecular mechanisms underlying the decline in neurons and impairment of cognitive function remain poorly understood.

Phospholipids participate in maintaining the integrity of cell membranes [9], regulating energy metabolism [10], and signal transduction [11] in neurons. iPLA2β (also known as PLA2G6) is a member of the phospholipase A2 superfamily, responsible for hydrolyzing glycerophospholipids at the sn-2 position to release lysophospholipids and fatty acids [12]. iPLA2β participates in phospholipid remodeling by regulating the concentration of polyunsaturated fatty acids in phospholipid stores [9]. For instance, inhibition of iPLA2β led to an elevation in arachidonic acid (AA)-containing phosphatidylcholine (PC) when cells were treated in culture [13]. Mutations in *iPLA2β* are associated with atypical neuroaxonal dystrophy (aNAD) [14], infantile neuroaxonal dystrophy (INAD) [15], and dystonia-Parkinsonism [16]. Whole-body iPLA2β-null mice exhibit weight loss with age-related neuroaxonal dystrophy [17], which is associated with disturbed brain phospholipids [18]. iPLA2β expression reduction by inserting an AP element impairs the function of the vesicle transport complex retromer in the Drosophila brain, resulting in an elevation of ceramides and neuronal impairment [19]. iPLA2β deficiency leads to shorter phospholipid acyl chains, which accelerate the aggregation of α-syn in neurons [19]. These findings indicate that iPLA2β may play a role in neuronal impairment during brain aging.

Mitochondria generate ATP via the tricarboxylic acid cycle and oxidative phosphorylation to meet the high-energy demands of the brain [20]. Loss of iPLA2β or its mutants results in decreased membrane potential, irregular mitochondrial structure, and reduced ATP synthesis in both the Drosophila brain and dopaminergic cell line SH-SY5Y [21]. PLA2G6 deficiency leads to gradual deterioration of the mitochondrial inner membrane and abnormal mitochondrial accumulation [22]. Mitophagy removes damaged mitochondria from neurons to maintain mitochondrial quality in healthy brains [23]. During the aging process, impaired mitophagy results in the overaccumulation of abnormal mitochondria, which is linked to neurodegenerative disorders [24]. Mitochondrial phospholipids are essential for maintaining the membrane integrity and functionality of respiratory chain enzymes, mtDNA biogenesis, and mitophagy [25]. Cardiolipin externalization to the outer mitochondrial membrane triggers mitophagy, facilitating the clearance of damaged mitochondria from neurons [26]. However, it remains unclear whether iPLA2β is associated with impaired mitophagy during brain aging.

We previously reported that iPLA2β$^{-/-}$ mice are prone to liver and intestinal injury, with increased inflammation and disruption of phospholipid metabolism during aging [27]. We hypothesized that iPLA2β is involved in age-related neuronal damage and cognitive decline. Here, we compared the extent of age-related cognitive decline in 24-month-old female wild-type and iPLA2β$^{-/-}$ mice. In addition to the changes in PFC phospholipids and impaired cognitive function observed in aged KO mice, our findings indicate that the brain is particularly vulnerable to aging sensitization in the absence of iPLA2β, primarily due to disrupted mitophagy. This disruption leads to increased neuronal apoptosis and inflammation. Our findings imply that genetic deficiency of iPLA2β can worsen age-related cognitive decline by disrupting neuronal mitophagy in the prefrontal cortex.

Materials and methods

Animals and treatment

iPLA2β knockout (iPLA2β$^{-/-}$) mice were generated by Shanghai Model Organisms Center, Inc. All animal experiments followed protocols approved by the Institutional Ethics Committee of the Chinese Academy of Medical Sciences and Peking Union Medical College. The mice were kept at the animal facility of the Chinese Academy of Medical Sciences with a12-h light–dark cycle and had free access to water and food. In our experiments, we used female iPLA2β$^{-/-}$ and C57BL/6J mice, aged 2–24 months. The mice were divided into four groups (n=20 per group): 2-month-old C57BL/6J, 24-month-old C57BL/6J, 2-month-old iPLA2β$^{-/-}$, and 24-month-old iPLA2β$^{-/-}$. For AAV injections, 22-month-old female C57BL/6J mice received stereotaxic injections into the prefrontal cortex with either iPLA2β AAV (1ul, 1×10^{13} V.G./mL) or control AAV (1ul, 1×10^{13} V.G./mL). The

mice were further divided into two groups ($n=20$ per group) based on the type of AAV injected: control AAV and iPLA2β-AAV. The injections were administered using the following stereotaxic coordinates: AP 2.7, ML+1.8, DV 2.0; AP 2.7, ML -1.8, DV 2.0. AAV injections were administered 21 days prior to formal behavioral testing [28]. Behavioral test training sessions were conducted two days before the formal testing began. Samples were collected on the 7th day following the initiation of the formal behavioral experiment. Figure 8a depicts the experimental design timeline, including the key time points for the assays and manipulations. The same set of animals was used for both Western Blot and PCR analyses to ensure consistency and comparability of results. Animals used for histology, including immunohistochemistry and immunofluorescence staining, were randomly selected from the same cohort as those used for Western blot and PCR.

Primary neurons culture

Primary neurons were isolated from the cortex of C57BL/6J mice on day 17 following the method outlined by Liu et al. [29]. For the D-gal (Sigma-Aldrich)-induced senescence model, primary neurons were cultured with 20 mg/mL D-gal in the culture medium for 48 h; For lentivirus mediated iPLA2β overexpression, purified lentivirus virus (2 μl, 4×10^8 TU/ml) was added to the culture medium for transduction.

Behavioral procedures

Morris water maze

The Morris water maze test was performed according to an established method [30]. Specifically, the test used a black circular pool divided into four quadrants (NE, NW, SE, and SW) and filled with water to a depth of 30 cm. A 10 cm platform was submerged 2 cm below the water surface and placed in the NE quadrant. Talcum powder was added to change the color of the water to white, facilitating the capture of images of the black mice using a camera. The water temperature was maintained constant from 23 °C to 25 °C throughout the experiment. The mice were subjected to five consecutive training trials. On the sixth day, a probe trial was conducted wherein the platform was removed and the mice were allowed to swim for 60s. Behavioral observations were captured using a camera positioned above the circular pool, and data analysis was performed using ANY maze software (SANS Biotechnology Co., Ltd).

Novel object recognition test

Novel object recognition test was conducted following the methods outlined in a published paper [28]. Each mouse underwent a 5-minute period of free exploration in an open-field box measuring 48×48 cm before formal testing. During the initial phase of the test, a cube-shaped object was placed within the box, and the mouse was given a 5-minute period for free exploration. Subsequently, a novel spherical object was introduced, and the mouse was given another 5 min to freely explore both objects. The time spent by the mice to investigate each object was recorded.

Elevated plus maze

The elevated plus maze test was conducted following the protocol outlined in a published paper [31]. Each mouse was positioned towards one of the open arms in the central connecting area and allowed to explore freely for 5 min. The time spent and number of entries into the open arms were recorded.

Rotarod test

Each mouse underwent adaptation training (SANS Biotechnology Co., Ltd.) before the formal experiment. During the formal test, the rotational speed of the rod was initially set to 5 rpm for 15 s, followed by a gradual increase to 50 rpm over a period of 5 min. Each mouse performed three repeat trials per session, with a 5-minute interval between trials for rest, and the average latency time of the three trials was recorded.

Adeno-associated virus production

The Pla2g6 sequence was inserted into the pAAV2-CMV_bGl-MCS-EGFP-WPRE-pA vector (Taitool Bioscience, Shanghai, China) to construct pAAV2-CMV_bGl-Pla2g6-2xFlag-HA-WPRE-SV40pA. The AAV9-Pla2g6 virus was generated by transfecting the overexpression construct and helper plasmids into AAV-293 cells. The AAV9-Pla2g6 virus was produced and purified using a modified standard protocol [32]. AAV9-CMV_bGI-EGFP-WPRE-pA (Taitool Bioscience, Shanghai, China) was used as control.

ATP level measurement

ATP levels were assessed using an ATP assay kit (Beyotime, S0026B) according to the manufacturer's instructions. Briefly, the tissue or cell lysates were centrifuged at 12,000 × g for 5 min, and the resulting supernatant was used for analysis. Protein concentration was determined using a BCA kit (CWBIO, CW0014S).

Histology, immunohistochemistry (IHC) and immunofluorescence staining

For brain paraffin sectioning, the mice were perfused with PBS. Brain specimens were fixed in 4% paraformaldehyde (PFA) for 48 h, embedded in paraffin blocks, and sectioned into 6 μm slices. The sections were subsequently stained with hematoxylin and eosin (H&E) for histological examination. For immunohistochemistry

(IHC), sections were deparaffinized and hydrated, followed by treatment with 10 mM citrate buffer (pH 6.0) and heating to boiling for 30 min. Endogenous peroxidase activity was blocked by treating the sections with 3% H_2O_2 for 10 min at room temperature. Then, brain sections were incubated overnight at 4 °C with the following antibodies: mouse polyclonal iPLA2β (sc-376563, 1:100, Santa Cruz), mouse monoclonal Iba1 (#17198, 1:400, Cell Signaling), or rabbit polyclonal GFAP (ab7260, 1:500, Abcam). Afterward, brain sections were incubated with anti-mouse and anti-rabbit secondary antibodies for 1 h at room temperature. Visualization of the protein/antibody complexes was achieved using DAB. The mPFC regions in the IHC sections were evaluated in a blinded manner. Histological changes were graded according to a previously described method [33]. The Histology score were graded in a blinded manner using a scoring system with the following criteria: Grade 0: Normal Limits-Tissue appears normal under the study conditions, accounting for factors such as age, sex, and strain. Any changes observed are within the expected range and are not considered pathological; Grade 1: Very Mild-Minimal changes are observed, just exceeding normal variation but with negligible pathological significance; Grade 2: Mild-Clear pathological lesions are present but are limited in extent and do not impair tissue function; Grade 3: Moderate-Pathological lesions are prominent and widespread, affecting tissue integrity and function; Grade 4: Severe-Extensive and severe pathological lesions, compromising the entire brain structure and function.

For brain cryosections used for immunofluorescence staining, mice were perfused with PBS, followed by 4% PFA. The brains were dissected and fixed in 4% PFA for 48 h. Subsequently, the brains were sequentially dehydrated in 15%, 20%, and 30% sucrose solutions, followed by embedding in OCT compound and sectioning into 10 μm slices [34]. For cell samples used in immunofluorescence staining, fixation was performed using 4% PFA for 15 min. Both brain sections and cells were permeabilized with 0.1% Triton X-100 in PBS, followed by incubation with primary antibodies at 4 °C overnight. Subsequently, sections and cells were incubated with Alexa-conjugated secondary antibodies for 1 h at room temperature before visualization. DAPI was applied for nuclear counterstaining. The primary antibodies employed in this study included iPLA2β (sc-376563, 1:100, Santa Cruz), NeuN (ab177487, 1:200, abcam), Iba1 (#17198, 1:400, Cell Signaling), GFAP (ab7260, 1:500, Abcam) and TOM20 (A19403, 1:200, ABclonal). The mPFC regions and cells on IF slides were evaluated in a blinded manner.

TUNEL staining

An In Situ Cell Death Detection Kit (Cat. #11684809910; Roche Applied Science) was used in this study. The sections were permeabilized with 1% Triton X-100 and 0.1% sodium citrate, followed by rinsing and staining according to the manufacturer's guidelines.

SA-β-gal staining

For animal experiments, the mice were perfused with PBS. The brains were dissected and embedded in OCT compound and sectioning into 20 μm slices. For fresh cell coverlids and brain slices, SA-β-gal staining was performed using a Senescence β-Galactosidase Staining Kit (#9860; CST). Briefly, brain sections or cells were fixed in a 1 × fixative solution for 15 min, followed by two rinses in 1X PBS. Brain sections or cells were immersed in Staining Solution and incubated at 37 °C. Subsequently, the cells were washed thrice with PBS, and the positive cells were observed under a microscope.

q-RT-PCR

Total RNAs was extracted using the Eastep® Super Total RNA Extraction Kit (cat#LS1040, Promega). Reverse transcription was performed using the GoScriptTM Reverse Transcription Mix kit (cat#A2800, Promega). q-RT-PCR was performed utilizing the GoTaq® qPCR Master Mix (cat#A6001, Promega) on a Bio-Rad CFX96 TOUCH instrument. q-RT-PCR was performed using the SYBR green method as we previously described [27]. The expression levels of the target genes were evaluated by the Δ–Ct method and normalized to Gapdh. The specific primers were used: mouse Gapdh (NM_001289726.2)-forward: 5′- TGTGTCCGTCGTG GATCTGA-3′, -reverse: 5′- TTGCTGTTGAAGTCGC AGGAG-3′; mouse iPLA2β/ Pla2g6 (NM_016915)-forward: 5′-AGATGTCTTTCGTCCCAGCA-3′, -reverse: 5′- ATGATGTCGGACCCTAGCTG-3′; mouse sPLA2/ Pla2g2a (NM_001082531)-forward: 5′-GGCTGTGTCA GTGCGATAAA-3′, -reverse: 5′- TTTGGGCTTCTTCC CTTTGC-3′; mouse iPLA2γ/ Pnpla8 (NM_026164)-forward: 5′-TCGGTGGTTACATTGGTGGA-3′, -reverse: 5′- GCTGAAGTAGCACACGCTTT-3′; mouse TGF-β (NM_011577)-forward: 5′- GGCTACCATGCCAACT TCTG-3′, -reverse: 5′- CGTAGTAGACGATGGGCAG T-3′; mouse TNF-α (NM_013693.3)-forward: 5′-CCAAC GGCATGGATCTCAAA-3′, -reverse: 5′-CCCTTGAAG AGAACCTGGGA-3′; mouse IL-1β (NM_008361.4)-forward: 5′- ACTCATTGTGGCTGTGGAGA-3′, -reverse: 5′- AGCCTGTAGTGCAGTTGTCT-3′; mouse CCL2 (NM_011333.3)-forward: 5′- GCTGGAGAGCTACAAG AGGA-3′, -reverse: 5′- ACCTTAGGGCAGATGCAGT T-3′.

Western blot analyses

Cells were homogenized in RIPA buffer (CW2333, CWBIO) and gently pipetted or vortexed to ensure complete cell lysis. Mice were anesthetized, and their brains were extracted and placed in ice-cold PBS. Brains were dissected to isolate the prefrontal cortices. The prefrontal cortices were specifically dissected and homogenized in RIPA buffer (CW2333, CWBIO) with a tissue homogenizer (KZ-III-F, Sercevio). Homogenized samples were then incubated on ice for 30 min. Following centrifugation at 13,000 × g for 10 min, the supernatant was collected. Protein concentrations were determined using the BCA Protein Assay Kit (CW0014S, CWBIO) and protein concentrations were between 3 and 5 ug/ul. Approximately 20 μg of sample proteins underwent 8–12% SDS-PAGE gel electrophoresis and were subsequently transferred onto PVDF membranes (Bio-Rad, USA). After blocking with 5% non-fat milk solution, the blots were incubated overnight at 4 °C with primary antibodies and subsequently incubated with HRP-conjugated secondary antibodies for 1 h at room temperature. The primary antibodies employed in this study included iPLA2β (#sc-376563, 1:200, Santa Cruz), P62(#5114, 1:1000, Cell Signaling), P16(#29271, 1:1000, Cell Signaling), Optineurin (#70928, 1:1000, Cell Signaling), PINK(23274-1-AP, 1:500, Proteintech), Parkin (#2132, 1:1000, Cell Signaling), Tom40 (sc-365467,1:500, Santa Cruz), MFF (#84580, 1:1000, Cell Signaling), LC3B (#83506, 1:1000,Cell Signaling), BNINP3(#3769, 1:1000,Cell Signaling), Nix (#12396, 1:1000, Cell Signaling), and β-actin (#4967, 1:1000, Cell Signaling). The protein bands were visualized using an ultrasensitive ECL chemiluminescence detection kit (PK10003, Promega) and captured using a ChemiDocTM Touch Imaging System (Bio-Rad, USA). ImageJ software was used to analyze the density of the protein bands (WB raw blots are provided in Additional file 10).

Transmission electron microscopy

Fresh mouse frontal cortex tissue samples (1 mm × 1 mm × 1 mm) were placed in fixation solution (0.1 M Phosphate Buffer containing 2.5% glutaraldehyde and 2.0% paraformaldehyde) and fixed at 4 °C for 4 h. After being washed three times with 0.1 M phosphate buffered saline, the frontal cortex tissues were post-fixed with 1% osmium tetroxide for 2 h. The tissue was rinsed three times with 0.1 M Phosphate Buffer for 15 min each. Dehydration was carried out by sequential immersion in 50%, 70%, 80%, 90%, 95%, and 100% ethanol, followed by 100% acetone for 15 min each. The tissue was then infiltrated with a series of mixtures of acetone and Epon 812 resin and finally embedded in pure Epon 812 resin. Ultrathin sections of the embedded samples were obtained using an ultramicrotome. The sections were double-stained with uranyl acetate and lead citrate and air-dried overnight. Observations and image acquisition were performed using a transmission electron microscope (HITACHI HT7800, Japan).

GFP-LC3 and Mito-DsRed analyses

48 h after transfection with AAV9-Pla2g6 or AAV9-CMV_bGI-EGFP-WPRE-pA, the primary cultured neurons were incubated in neurobasal FBS containing 20 mg/ml D-gal for 48 h. Next, neurons were transfected with AAVs containing GFP-LC3B and Mito-DsRed and allowed to recover for 48 h in growth media.

LC-MS/MS analysis

Lipidomic analysis was performed using an established protocol [35] (Biotree, Shanghai, China). For lipid extraction, 10 mg of the brain sample was homogenized in 400 μL H2O. Subsequently, the extract solutions were added to the brain homogenates and mixed thoroughly. The mixtures were centrifuged, and the supernatants were collected. An equivalent amount of MTBE was added to the supernatant, which was sonicated and centrifuged to isolate the supernatant. The supernatant was evaporated under vacuum and reconstituted. LC-MS/MS analysis was performed using a UHPLC system (1290, Agilent Technologies) with an ACQUITY UPLC HSS T3 column (1.8 μm, 2.1×100 mm). Biobud-v2.0.7 Software was used for quantification.

Statistics

Statistical analyses were performed using GraphPad Prism version 8. Results are presented as the mean ± SEM. Normality of data distribution was assessed using the Shapiro–Wilk normality test. For normally distributed data, comparisons between two groups were performed using a two-tailed Student's t-test with Welch's correction ($^{*}p<0.05$, $^{**}p<0.01$, $^{***}p<0.001$). For non-normally distributed data, comparisons between the two groups were made using the Mann-Whitney U test. For comparisons involving more than two groups with normally distributed data, one-way analysis of variance (ANOVA) followed by Tukey's post hoc test was used. For non-normally distributed data involving more than two groups, the Kruskal-Wallis test followed by Dunn's multiple comparison test was applied ($^{*}p<0.05$, $^{**}p<0.01$, $^{***}p<0.001$).

Results

Aging increased iPLA2β loss in PFC of mice

The PFC (prefrontal cortex) is particularly susceptible to aging stress [8]. The process of phospholipid remodeling is critically important for maintaining phospholipid homeostasis in aging PFC. The phospholipase A2 superfamily is responsible for hydrolyzing glycerophospholipids at the sn-2 position and releasing lysophospholipids and fatty acids during this phospholipid

remodeling process [12]. To identify the members of the iPLA2 family that exhibited significantly altered expression levels in the aged PFC, we compared iPLA2 expression in the PFC of young and old mice. There was a notable decrease in iPLA2β mRNA levels in the aged PFC, whereas sPLA2, cPLA2, and iPLA2γ showed no significant changes compared to their younger counterparts (Fig. 1A). Next, we analyzed changes in iPLA2β protein levels during brain aging using Western blotting. We observed a significant decrease in iPLA2β expression in the PFC of aged mice (18-month-old and 24-month-old groups) compared to younger mice (2-month-old and 10-month-old groups) (Fig. 1B). However, no significant changes in iPLA2β protein expression were observed in the hippocampus of aged mice (Additional File.1 A-B). Consistently, immunohistochemical staining for iPLA2β revealed a decrease that correlated with age in the PFC of aged mice (Fig. 1C). iPLA2β exhibited significant colocalization with the neuronal marker NeuN, and its expression was significantly decreased in the neurons of aged mice (Fig. 1D). iPLA2β also showed some colocalization with the microglial marker Iba1, with a significant downregulation observed in microglial cells of aged mice. In contrast, iPLA2β exhibited limited colocalization with the astrocytic marker GFAP (Additional File 2 A, B).

Deficiency of iPLA2β in aged mice brain increases aging-related cognitive impairment and neuroinflammation

To investigate the role of iPLA2β in the PFC, we used iPLA2β knockout (iPLA2β$^{-/-}$) mice. Our results showed a significant reduction in iPLA2β mRNA levels (Fig. 2A), whereas sPLA2, cPLA2, and iPLA2γ levels remained unchanged (Additional File 3 A-C). Western blotting confirmed the absence of iPLA2β protein in the PFC of iPLA2β$^{-/-}$ mice (Fig. 2B). In the PFC of iPLA2β$^{-/-}$ mice, we observed a further decrease in cell density, increased nuclear wrinkling and condensation, neuronal death, and neuronal vacuole formation compared to 24-month-old wild-type (WT) mice (Additional File 4 A). To assess the effect of iPLA2β deficiency on age-related cognitive decline, we performed a Morris water maze test. Compared with younger controls, 24-month-old mice took significantly longer to find the hidden platform, made fewer platform crossings, and spent less time in the target quadrant. Aged iPLA2β-deficient mice showed greater impairments than aged wild-type mice, with longer latencies to find the hidden platform, fewer platform crossings, and reduced time in the target quadrant (Fig. 2C-E; Additional File 5 A). To ensure that the observed cognitive deficits were not influenced by motor or anxiety-related factors, we conducted additional behavioral tests. The rotarod test, which assesses motor coordination [36], indicated that aged iPLA2β-deficient mice had

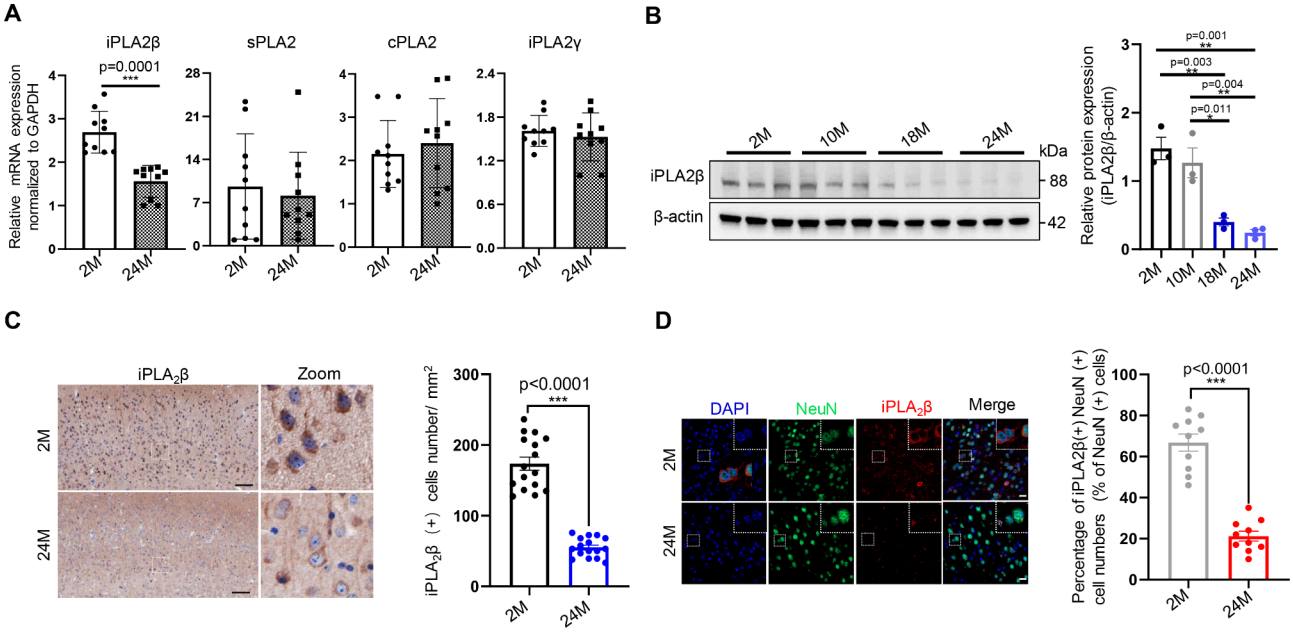

Fig. 1 Aging increased iPLA2β loss in the PFC of mice. **A** PLA2s mRNA expression levels in the PFC were assessed using qPCR. Normalization was conducted relative to GAPDH expression levels. $n=10$. **B** iPLA2β protein levels in the PFC were assessed via Western blotting. $n=3$. **C** Representative IHC images depicting iPLA2β in the PFC. IHC analysis showing the density of iPLA2β (+) cells/mm^2. Scale bar: 100 μm. $n=16$. **D** Representative immunofluorescence images depicting iPLA2β (red) and NeuN (green) in the PFC. The bar graph shows the percentage of iPLA2β(+) NeuN(+) cells relative to the total NeuN(+) cell population (%).Scale bar: 20 μm. $n=10$

M represents "month" Data are presented as mean ± SEM; *p* values were obtained using Mann-Whitney U test (A), one-way analysis of variance (ANOVA) followed by Tukey's post hoc test (B), and two-sided unpaired Student's t-tests (C, D). * $p<0.05$. **, $p<0.01$; ***, $p<0.001$

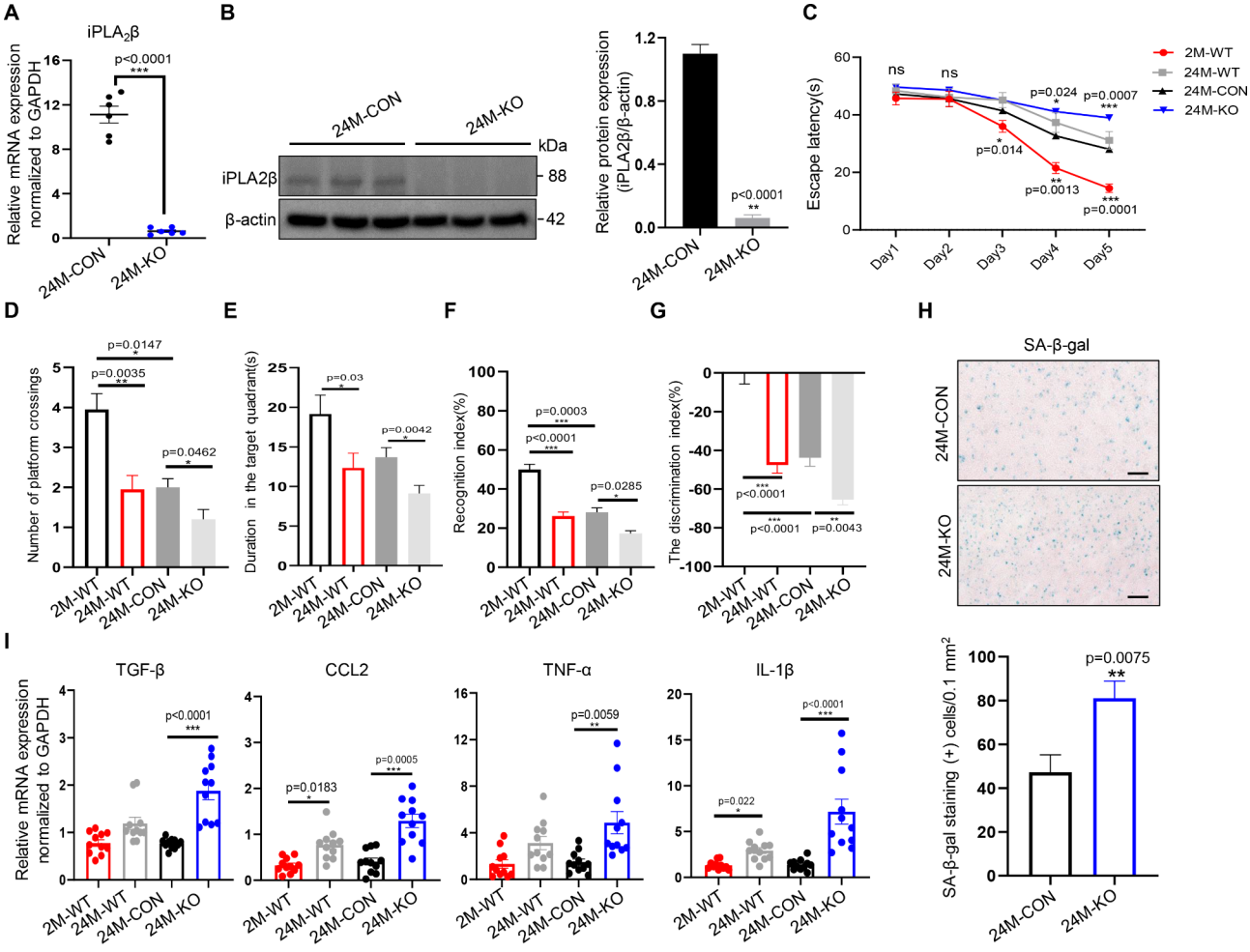

Fig. 2 Deficiency of iPLA2β increases aging-related cellular senescence, cognitive impairment and neuroinflammation. **A** The mRNA expression levels of iPLA2β in the PFC of 24 M mice were assessed by qPCR. Normalization was performed relative to GAPDH expression levels. $n=6$. **B** Protein levels of iPLA2β in the PFC of 24 M mice, assessed using Western blotting and densitometry, $n=3$. **C** Time taken by 2 M-WT, 24 M-WT, 24 M-CON, and 24 M-KO mice to reach the platform during the spatial test. $n=20$. **D** Frequency of platform crossings in 24 M mice during the probe trial. $n=20$. **E** Duration of 2 M-WT, 24 M-WT, 24 M-CON, and 24 M-KO mice spent time in hidden platform quadrants during the probe trial. $n=20$. **F** Recognition index of 2 M-WT, 24 M-WT, 24 M-CON and 24 M-KO mice during the Novel object recognition test. Recognition index = time spent exploring novel object/time spent exploring both objects. $n=20$. **G** The discrimination index of 2 M-WT, 24 M-WT, 24 M-CON, and 24 M-KO mice during the Novel object recognition test. The discrimination index = (time spent on the novel object − time spent on the familiar object)/ time spent on both objects. $n=20$. **H** Representative SA-β-gal staining images in 24 M PFC. The bar graph shows the density of β-Gal staining (+) cells/0.1 mm^2. Scale bar: 100 μm. $n=10$. **I** mRNA levels of TGF-β, CCL2, TNF-α, and IL-1β in the PFC of 2 M-WT, 24 M-WT, 24 M-CON, and 24 M-KO mice were assessed via qPCR. Normalization was conducted relative to GAPDH expression levels. $n=11$

KO represents "iPLA2β knockout," CON represents "control", Data are presented as mean ± SEM; *p* values were obtained using two-sided unpaired Student's t-tests (A, B, H), the Kruskal-Wallis test followed by Dunn's multiple comparisons test (C, D, E, F, G and I), * $p<0.05$. **, $p<0.01$; ***, $p<0.001$

similar motor performance to their wild-type counterparts (Additional File 5 C). Furthermore, the elevated plus maze, used to evaluate anxiety levels [37], showed no significant differences between the two groups (Additional File 5D-E). Additionally, the swimming speed of iPLA2β-deficient mice was comparable to that of wild-type mice (Additional File 5 B). In the novel object recognition test, iPLA2β-deficient aged mice showed further reduced exploration of novel objects compared to younger controls, as indicated by their lower discrimination and recognition indices (Fig. 2F-G). These findings indicate that iPLA2β is associated with age-related brain pathology and cognitive decline.

iPLA2β deficiency was associated with increased SA-β-gal activity in the aged PFC (Fig. 2H), indicating elevated cellular senescence [38]. TUNEL-positive cells were also notably higher in the iPLA2β$^{-/-}$ PFC compared to wild-type controls (Additional File.4 B). qPCR analysis revealed significant upregulation of inflammatory cytokines and chemokines, including TGF-β, TNF-α, IL-1β, and CCL2, in the iPLA2β$^{-/-}$ PFC compared to wild-type controls (Fig. 2I). This indicates a notable inflammatory

response associated with iPLA2β deficiency. Additionally, our data show that iPLA2β deficiency exacerbates astrogliosis and microgliosis during PFC aging, as evidenced by the increased numbers of Iba1(+) and GFAP (+) cells (Additional File 6). While astrogliosis [39] and microgliosis [40] naturally increase with age, the exacerbation observed in iPLA2β-deficient mice underscores the role of iPLA2β in modulating neuroinflammation.

iPLA2β reduces senescence in primary neurons

Neuronal senescence is closely associated with brain aging and is characterized by dysfunctional mitochondria, increased SA-β-gal levels, and upregulation of cell cycle inhibitors [41]. To explore the role of iPLA2β in neuronal senescence, we first assessed iPLA2β expression in long-term cultured mouse primary cortical neurons, which served as a neuronal senescence model as previously described [28]. In long-term cultured neurons (20 days in vitro [DIV20]), we observed a significant reduction in iPLA2β mRNA levels (Fig. 3A), and protein (Fig. 3B) levels compared to young controls (DIV7). Consistently, iPLA2β overexpression significantly reduced the number of β-gal-expressing neurons in the long-term culture (Fig. 3C). D-galactose (D-gal) was used to establish an aging cell model because of its ability to induce oxidative stress and mimic age-related changes [42]. A D-gal-induced neuronal aging model was used to confirm the role of iPLA2β in neuronal senescence. Immunofluorescence results indicated a decrease in iPLA2β expression in D-gal-treated groups (Fig. 3D). D-gal treatment significantly increased the number of SA-β-gal-stained neurons (Fig. 3E). Overexpression of iPLA2β significantly reduced the number of SA-β-gal-stained neurons following D-gal treatment (Fig. 3E). Following D-gal treatment, iPLA2β overexpression significantly decreased P16 expression and increased P62 expression compared to the control (Fig. 3F).

iPLA2β protects mitochondrial morphology and regulate mitochondrial function during brain aging

Mitochondrial homeostasis is critical for maintaining neuronal function during the aging process [43]. Transmission electron microscopy (TEM) was performed to explore the effect of iPLA2β on mitochondrial function. As shown in Fig. 4A, the 24 M iPLA2β$^{-/-}$ cortex displayed more severe mitochondrial swelling, matrix dissolution, cristae rupture, and vacuolization than the 24 M WT control (Fig. 4A). Conversely, iPLA2β overexpression in the cortex of 24-month-old mice partially mitigated mitochondrial damage observed in the aged cortex (Fig. 4B). Quantitative analysis revealed that iPLA2β knockout resulted in an increase in mitochondrial diameter (Fig. 4C, D), whereas iPLA2β overexpression reduced age-related mitochondrial diameter and length in the cortex of aged mice (Fig. 4E, F). Additionally, ATP synthesis decreased in the cortex of iPLA2β$^{-/-}$ mice (Fig. 4G), whereas iPLA2β overexpression increased ATP levels in the aged cortex (Fig. 4H). To further explore the association between iPLA2β and mitochondrial damage, we examined the colocalization of iPLA2β and the mitochondrial membrane protein TOM20 in the cortex. The results demonstrated that iPLA2β and TOM20 colocalized in the cortex of mice (Fig. 4I), with aging leading to significant downregulation of both iPLA2β and TOM20. In aged mice, iPLA2β overexpression resulted in a further decrease in TOM20 levels. This suggests that iPLA2β overexpression may modulate TOM20 expression, potentially impacting mitochondrial quality control processes, such as mitophagy (Fig. 4J-K). These findings imply a protective role for iPLA2β in maintaining mitochondrial function during cortical aging.

iPLA2β regulates mitophagy during neuronal aging in vivo and in vitro

Mitochondrial dysfunction during brain aging is often accompanied by disrupted mitophagy [44]. We investigated whether iPLA2β deficiency PFCs exhibit a decrease in mitophagy by assessing the ratio of mitochondrial to nuclear DNA (mtDNA: nDNA). Indeed, mtDNA: nDNA was increased in iPLA2β-KO PFCs compared to that in the 24 M controls (Fig. 5A). Markers associated with PINK1/Parkin-dependent and -independent pathways are significantly altered in the aged nervous system of mice [45]. To elucidate the mechanism by which iPLA2β triggers mitophagy, we examined the involvement of these pathways in the mitochondrial fractions isolated from aged PFCs. iPLA2β deficiency resulted in the accumulation of Parkin, PINK1, and Optineurin, along with decreased levels of the mitochondrial fission factor MFF and downregulation of the autophagy marker LC3B (Fig. 5B). Conversely, iPLA2β overexpression PFCs showed decreased mtDNA: nDNA (Fig. 5D), protein levels of mitochondrial Parkin and PINK1, mitochondrial fission factor MFF, and autophagy marker LC3B, indicating a role for Parkin-dependent mitophagy (Fig. 5E). Moreover, iPLA2β overexpression/knockout did not lead to significant alterations in BNIP3 and NIX levels (Fig. 5C, F), indicating the absence of parkin-independent mitophagy pathways [46].

A D-gal-induced neuronal aging model was used to confirm the role of iPLA2β in mitophagy during neuronal senescence. Primary cultured neurons were transfected with plasmids expressing GFP-LC3B and Mito-DsRed, and mitophagy was quantified using the ratio of LC3B puncta with mitochondria. Following D-gal treatment, the ratio of LC3B puncta with mitochondria was significantly reduced in neurons compared to that in PBS-treated controls. However, iPLA2β overexpression significantly increased this ratio compared to that in the control group following D-gal treatment (Fig. 6A, B). Such colocalization was further

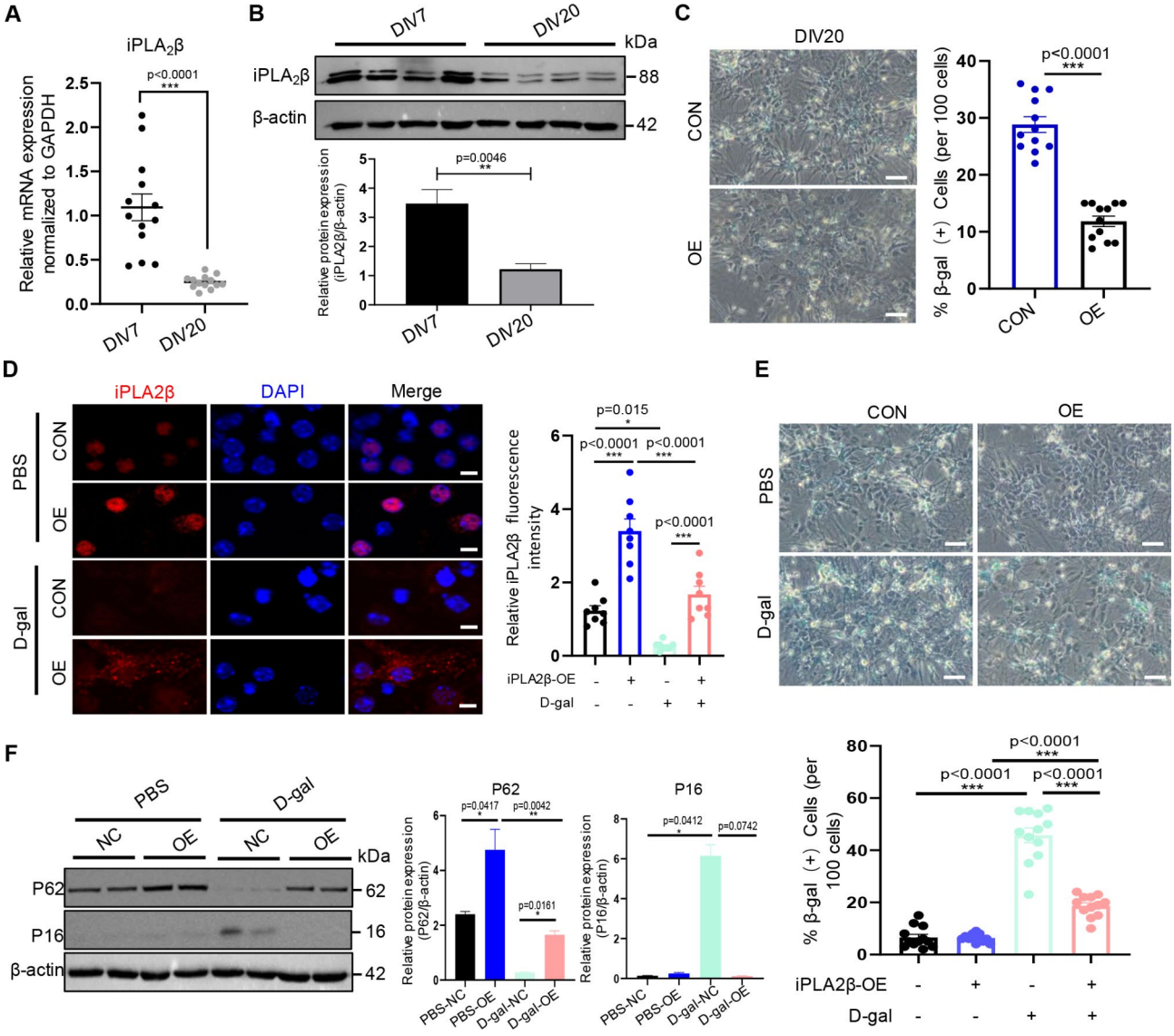

Fig. 3 iPLA2β reduces senescence in primary neurons. **A** The mRNA levels of iPLA2β in DIV7 and DIV20 cultured neurons were assessed using qPCR. Normalization was conducted relative to GAPDH expression levels. $n = 13$. **B** Protein levels of iPLA2β in DIV7 and DIV20 cultured primary neurons, assessed via Western blot and densitometry. $n = 4$. **C** Representative SA-β-gal staining images of iPLA2β-overexpression (OE) and control DIV20 primary neurons. Scale bar: 100 μm. $n = 12$. **D** Representative immunofluorescence images of iPLA2β (red) in D-gal-induced iPLA2β overexpression (OE) and control primary neurons. Scale bar: 5 μm. $n = 8$. **E** Representative SA-β-gal staining images of D-gal-induced iPLA2β-overexpression (OE) and control primary neurons. Scale bar: 100 μm. $n = 12$. **F** Protein levels of P62 and P16 in D-gal-induced iPLA2β-overexpression (OE) and control primary neurons, as assessed by Western blot and densitometry

OE represents "iPLA2β overexpression", CON represents "control", Data are mean ± SEM; *p* values were obtained using two-sided unpaired Student's t-tests (A, B), Mann-Whitney U test (C), one-way analysis of variance (ANOVA) followed by Tukey's post hoc test (E), the Kruskal-Wallis test followed by Dunn's multiple comparisons test (F), * $p < 0.05$. **, $p < 0.01$; ***, $p < 0.001$

enhanced when D-gal was co-treated with the autophagy inhibitor chloroquine (CQ) (Fig. 6A, B), which may have prevented the degradation of colocalized LC3B-mitochondria [47]. Conversely, iPLA2β knockout neurons showed a decreased ratio of colocalized LC3B-mitochondria compared to the controls (Additional File.7 A-B). Additionally, after D-gal induction, iPLA2β overexpression increased the levels of mitochondrial Parkin, Optineurin, and PINK1 (Fig. 6C), and elevated levels of MFF and LC3B (Fig. 6D). These results indicate that iPLA2β plays a protective role in mitophagy during neuronal aging.

iPLA2β deficiency leads to alterations in mitochondrial phospholipid metabolism in aged PFC

Phospholipids are crucial for maintaining the brain microenvironment and ensuring normal mitochondrial structure and function, with lipid influx being essential for cognitive function [48]. Evidence suggests that

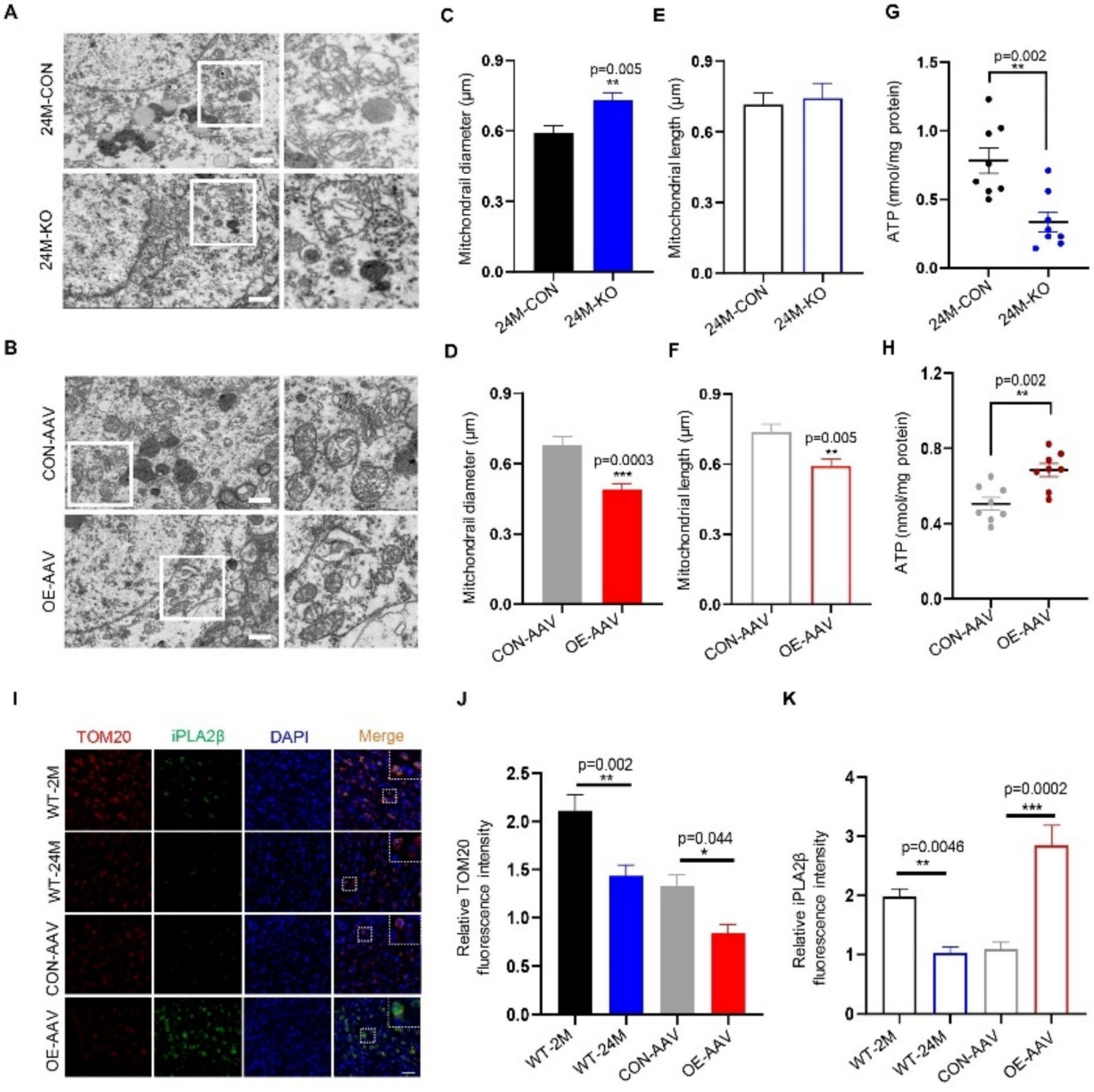

Fig. 4 iPLA2β protects mitochondrial morphology and regulate mitochondrial function during cortex aging. **A** Representative TEM image of WT and iPLA2β$^{-/-}$ PFC of 24 M mice. Scale bar: 1 μm. **B** Representative TEM images of the AAV-CON-injected and AAV-iPLA2β-OE-injected PFC of mice. Scale bar: 1 μm. **C** Quantification of mitochondrial diameter in TEM images of WT and iPLA2β$^{-/-}$ PFC from 24 M mice. $n = 10$. **D** Quantification of mitochondrial diameter in TEM images of the AAV-CON-injected and AAV- iPLA2β-OE-injected PFC of mice. n = 10.**E** Quantification of mitochondrial length in TEM images of WT and iPLA2β$^{-/-}$ PFC from 24 M mice. $n = 10$. **F** Quantification of mitochondrial length in TEM images of the AAV-CON-injected and AAV-iPLA2β-OE-injected PFC of mice. $n = 10$. **G** ATP levels in the WT and iPLA2β$^{-/-}$ PFC of 24 M mice. $n = 8$. **H** ATP levels of the AAV-CON-injected and AAV-iPLA2β-OE-injected PFC of mice. $n = 8$. I Representative immunofluorescence images of iPLA2β (green) and TOM20 (red) in the PFC of 2 M-WT, 24 M-WT, AAV-CON-injected, and AAV- iPLA2β-OE-injected mice. Scale bar: 50 μm. **J** TOM20 fluorescence intensity of immunofluorescence images in (I). $n = 12$. **K** iPLA2β fluorescence intensity of immunofluorescence images in (I). $n = 12$

KO represents "iPLA2β knockout," WT represents "wildtype", OE represents "iPLA2β overexpression", CON represents "control", Data are mean ± SEM; *p* values were obtained using two-sided unpaired Student's t-tests (C, D, E, F, G, and H), the Kruskal-Wallis test followed by Dunn's multiple comparisons test (J and K), * $p < 0.05$. **, $p < 0.01$; ***, $p < 0.001$

mitochondria undergo age-related functional and morphological changes. We conducted lipidomic analysis to examine the profiles of mitochondrial phospholipids and lysophospholipids to evaluate the role of iPLA2β in brain

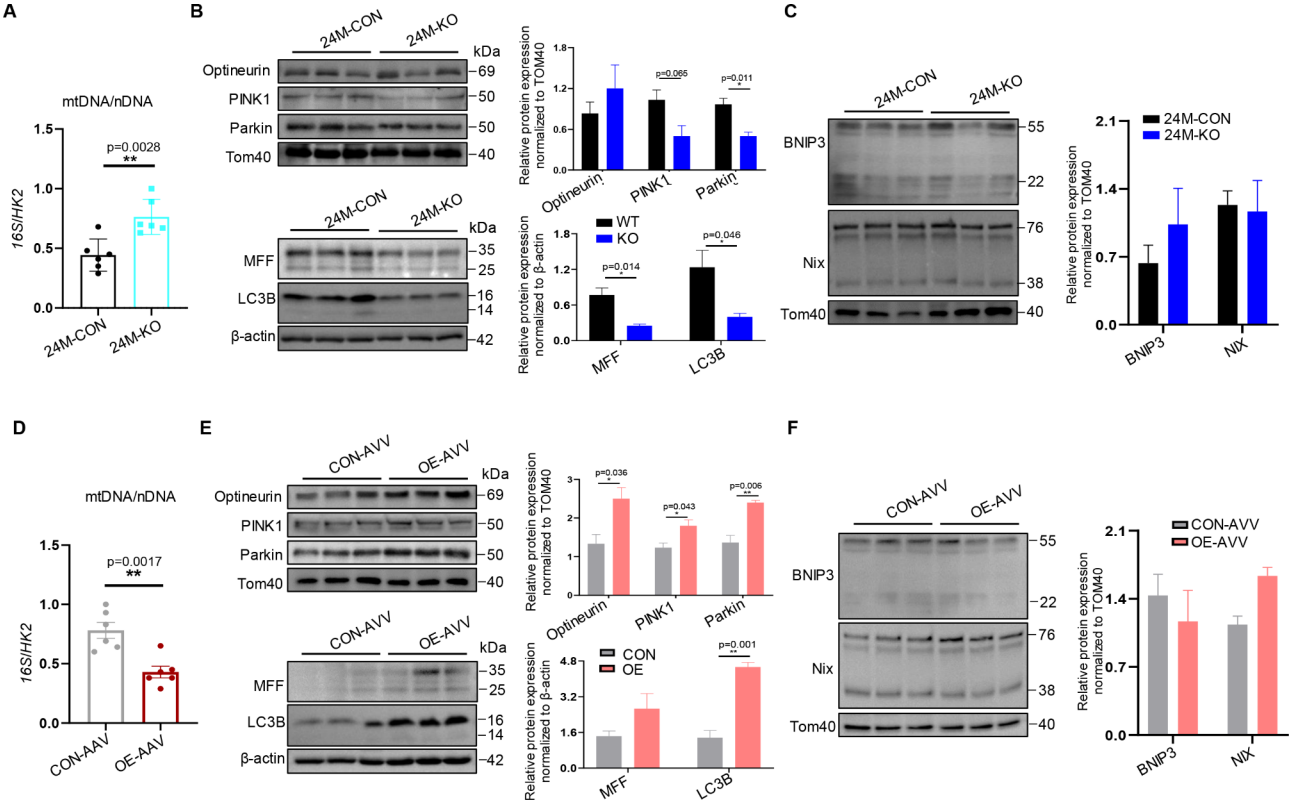

Fig. 5 iPLA2β regulates mitophagy during neuronal aging in vivo. **A** Quantification of the mtDNA/nDNA ratio in the 24 M PFC in the wild-type (WT) and iPLA2β knockout (iPLA2β$^{-/-}$) groups, using 16 S rRNA and Hexokinase 2 (Hk2), respectively. $n=6$. **B** Optineurin, PINK1, Parkin, MFF, and LC3B levels in the 24 M PFC in wild-type (WT) and iPLA2β knockout (iPLA2β$^{-/-}$) groups, assessed by Western blot and densitometry. $n=3$. **C** BNIP3 and NIX levels in the 24 M PFC in wild-type (WT) and iPLA2β knockout (iPLA2β$^{-/-}$) groups, assessed by Western blot and densitometry. $n=3$. **D** Quantification of the mtDNA/nDNA ratio in the 22 M PFC with iPLA2β overexpression (OE) and control (CON) groups, using 16 S rRNA and Hexokinase 2 (Hk2), respectively. $n=6$. **E** Optineurin, PINK1, Parkin, MFF, and LC3B levels in the 22 M PFC with iPLA2β overexpression (iPLA2β-OE) and control (CON) groups, assessed by Western blot and densitometry. $n=3$. **F** BNIP3 and NIX levels in the 22 M PFC with iPLA2β overexpression (iPLA2β-OE) and control (CON) groups, as assessed by Western blotting and densitometry. $n=3$

KO represents "iPLA2β knockout", WT represents "wildtype", OE represents "iPLA2β overexpression", CON represents "control", Data are presented as the mean ± SEM; *p* values were obtained using two-sided unpaired Student's t-tests (A, B, C, and D). * $p<0.05$. **, $p<0.01$; ***, $p<0.001$

aging. By comparing aged KO and WT PFCs, we found that the total level of lysophospholipids was reduced in aged KO PFCs (Fig. 7A, B). Previously, we demonstrated that male KO mice aged 20–22 months exhibited decreased intestinal iPLA2 activity and reduced levels of its product, LPC [27]. Consistently, the PFCs of aged female KO mice exhibited decreased MUFA-LPC and total LPC levels (Fig. 7A). For the individual species depicted in Fig. 7A, a moderate but significant decrease in LPC14:0 and LPC22:4 was detected in the PFCs of aged KO mice. In the comparison between aged KO and WT PFCs, there was a tendency towards lower levels of total and MUFA-LPE, with a notable decrease observed in saturated and PUFA-LPE (Fig. 7B). Among the PUFA-LPEs, LPE 22:5 was associated with a decrease in PE18:1/22:5. Additionally, a significant decrease of LPE18:0, LPE20:3, and LPE20:5 was observed in aged KO PFCs (Fig. 7B). PFCs of aged KO mice showed no significant alterations in PLs. Specifically, no significant changes were observed in PC/PE-containing saturated, MUFA, PUFA, or total PC/PE (Fig. 7C, D). However, specific changes were observed: a significant decrease in PC18:1/20:5, a tendency towards decreased levels of PE18:1/22:5 and PE18:1/18:3, and a notable increase in PC16:0/16:0 in aged KO PFCs (Fig. 7C, D). Therefore, iPLA2β deficiency results in changes in phospholipid metabolism in the aged PFCs.

Overexpression of iPLA2β in the PFC improves cognitive function in aged mice

iPLA2β was introduced into the PFC of 22-month-old female mice (Fig. 8A), which was chosen to ensure an effective AAV injection and minimize mortality. Overexpression of the iPLA2β protein was confirmed by Western blot (Fig. 8B). As shown in Fig. 8C, iPLA2β exhibited significant colocalization with the neuronal marker NeuN, and its expression was markedly upregulated in neurons (Fig. 8C). iPLA2β overexpression led

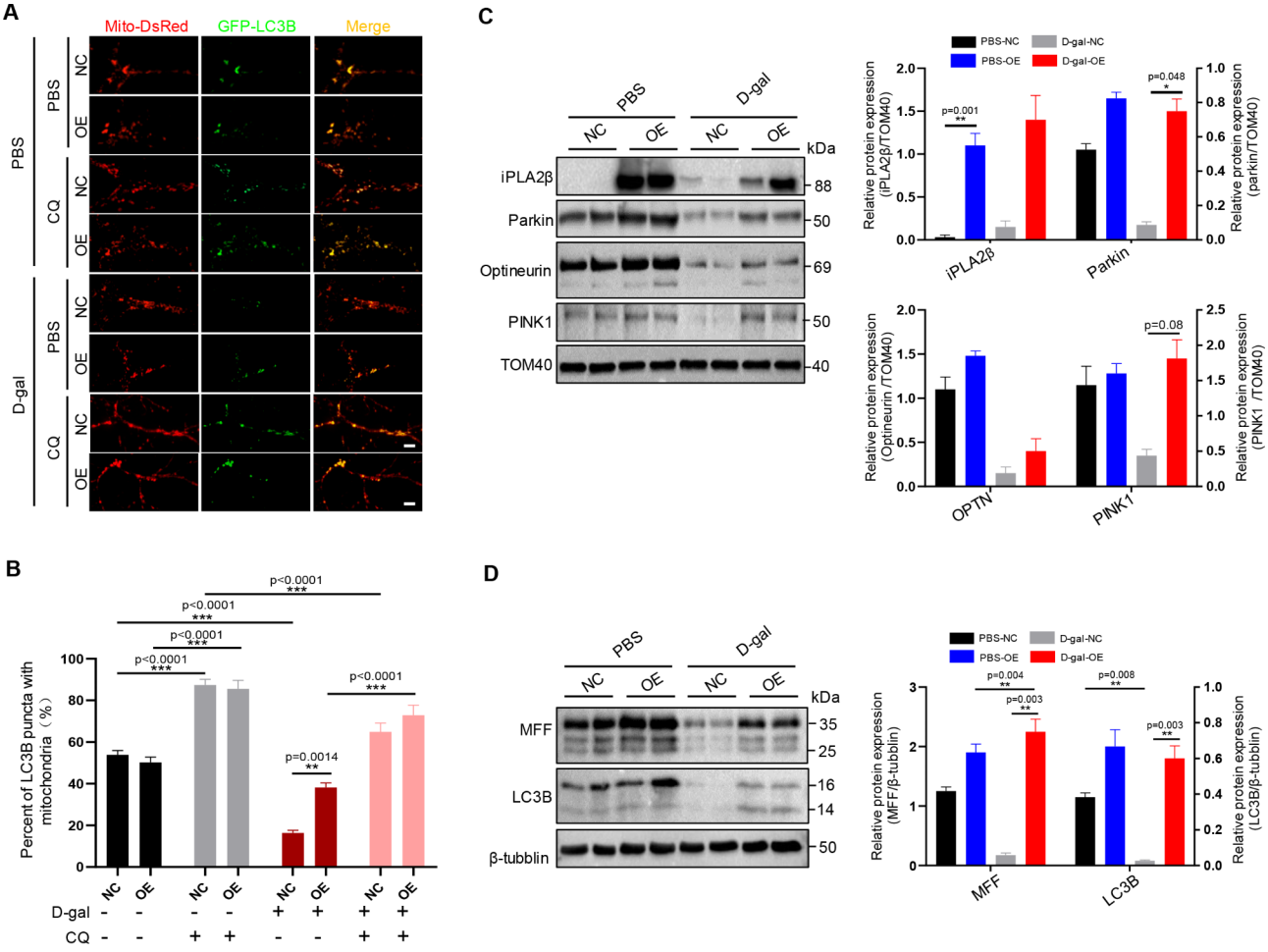

Fig. 6 iPLA2β regulates mitophagy during neuronal aging in vitro. **A** Primary cultured cortical neurons were transfected with GFP-LC3B and Mito-DsRed. Fluorescent images were captured 3 h after reperfusion. Scale bar: 5 μm. **B** Relative colocalization ratio between GFP-LC3B and Mito-DsRed in immunofluorescence images in (A). The ratio was calculated by dividing the number of LC3B-Mito puncta by the total number of Mito puncta. $n = 6$. **C** Mitochondrial levels of iPLA2β, Parkin, optineurin, and PINK1 were assessed by Western blot and densitometry in D-gal-induced iPLA2β overexpression (OE) and control primary neurons. **D** Protein levels of MFF and LC3B were evaluated using Western blot and densitometry in D-gal-induced iPLA2β overexpression (OE) and control primary neurons

CQ represents "chloroquine", D-gal represents "D-galactose", OE represents "iPLA2β overexpression", NC represents "Negative Control", Data are presented as the mean ± SEM; *p* values were obtained using, one-way analysis of variance (ANOVA) followed by Tukey's post hoc test (B), the Kruskal-Wallis test followed by Dunn's multiple comparisons test (C and D). * $p < 0.05$. **, $p < 0.01$; ***, $p < 0.001$

to a significant reduction in the number of SA-β-gal-positive cells in the aged PFC (Fig. 8D). Meanwhile, the mRNA expression levels of TGF-β, TNF-α, IL-1β, and CCL2 were significantly decreased in aged PFC with iPLA2β overexpression (Fig. 8E). Overexpression of iPLA2β alleviates astrogliosis and microgliosis during prefrontal cortex aging, as evidenced by a decrease in the number of Iba1(+) (Fig. 8F) and GFAP(+) cells (Additional File.8). Notably, behavioral assessments revealed that aged PFC with iPLA2β overexpression displayed significantly improved cognitive function (Fig. 8G-I). Aged mice overexpressing iPLA2β spent significantly less time finding the platform (Fig. 8G) and crossed the platform more frequently (Fig. 8H) and spent more time in the target quadrant (Fig. 8I) (Additional File 9 A). iPLA2β-Overexpression mice had similar swimming speed (Additional File 9 B), locomotor activity (Additional File 9 C), and anxiety levels (Additional File 9D-E) as their counterparts, excluding these factors from influencing the Morris water maze results. In the novel object recognition test, iPLA2β-Overexpression aged mice showed increased exploration of novel objects compared to younger controls, as indicated by their higher discrimination and recognition indices (Fig. 8J-K).

Discussion

The phospholipase A2 superfamily regulates cellular energy metabolism and signal transduction by hydrolyzing glycerophospholipids at the sn-2 position to release lysophospholipids and fatty acids, which are essential

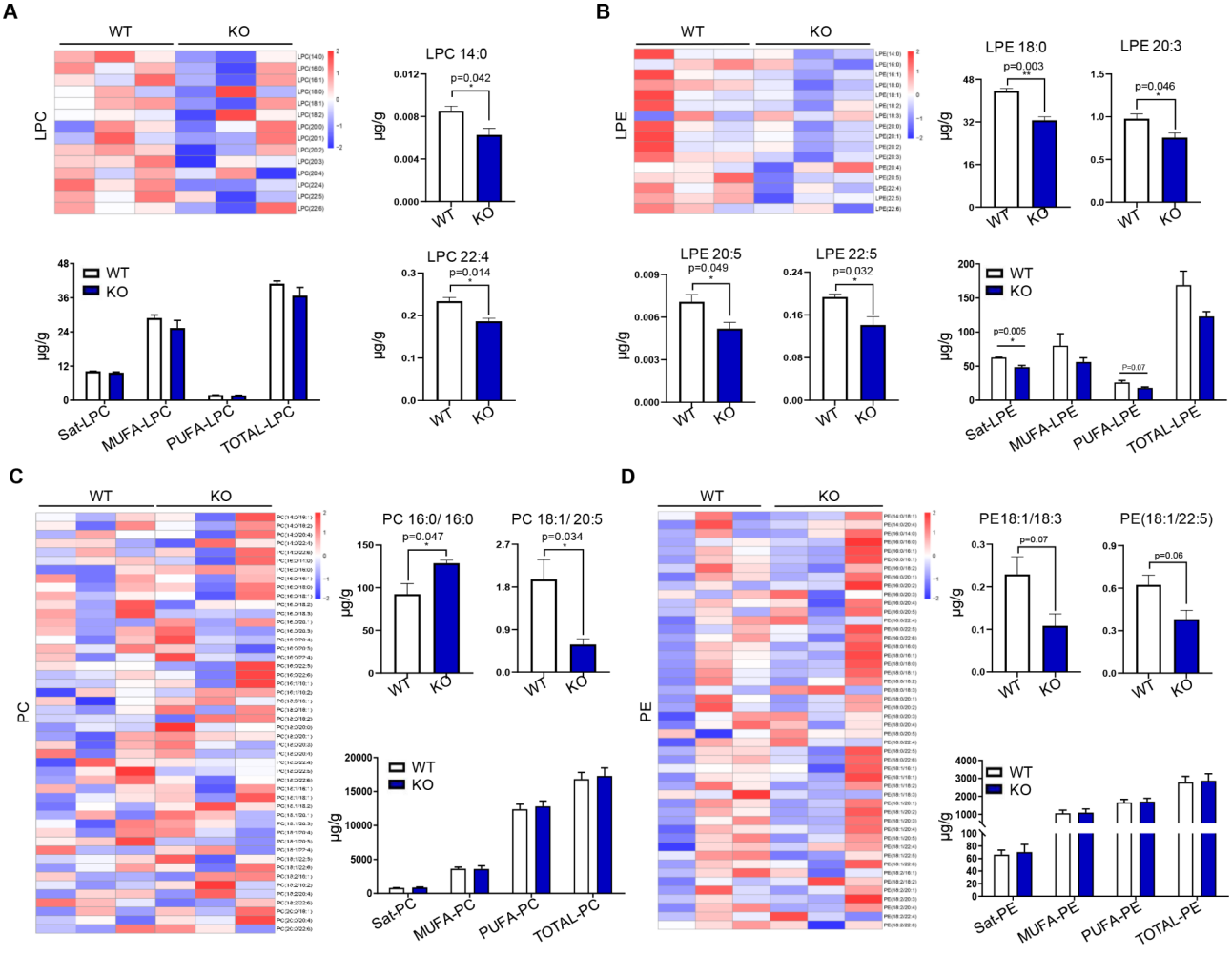

Fig. 7 iPLA2β deficiency leads to alterations in mitochondrial phospholipid metabolism in aged PFC. **A** Heat map representing individual LPC species and lipidomic analysis of LPC species were significantly altered in the KO group in 24 M PFCs. **B** Heat map representing individual LPE species and lipidomic analysis of LPE species significantly altered in the KO group in 24 M PFCs. **C** Heat map representing individual PC species and lipidomic analysis of PC species significantly altered in the KO group in 24 M PFCs. **D** Heat map representing individual PE species and lipidomic analysis of PE species significantly altered in the KO group in 24 M PFCs

MUFA represents "monounsaturated fatty acid"; PUFA represents "polyunsaturated fatty acid". Data are presented as the mean ± SEM; *p* values were obtained using two-sided unpaired Student's t-tests (A, B, C, and D). * $p < 0.05$. **, $p < 0.01$; ***, $p < 0.001$

for maintaining neuronal homeostasis [49]. The PFC is essential for complex cognitive tasks, especially those involving core functions, such as working memory. Nevertheless, the link between different PLA2 levels and brain aging remains uncertain, particularly within the prefrontal cortex, which is most vulnerable to age-related changes. In this study, we observed that reduced iPLA2β levels in aged PFCs may act as an intrinsic factor contributing to age-related cognitive impairment by influencing neuronal mitophagy. We provide the first evidence confirming the selective downregulation of iPLA2β, rather than other PLA2 family proteins (sPLA2, cPLA2, or iPLA2γ), in the PFC of aged mouse brains and cellular aging models. Loss of iPLA2β in the brains of aged mice increases age-related phenotypes, apoptosis, neuroinflammatory responses, and cognitive dysfunction, along with defective mitochondrial function induced by disrupted mitophagy and altered mitochondrial phospholipid profiling. Notably, iPLA2β overexpression mitigated age-related cognitive dysfunction by improving mitophagy in the aged PFCs. Collectively, our findings indicate that iPLA2β serves as a critical regulator of mitophagy and plays a protective role against age-related cognitive dysfunction.

The mechanism by which iPLA2β deficiency increases susceptibility to age-related injuries is an ongoing focus of our laboratory. This study was based on the link between the disruption of phospholipid metabolic homeostasis and the development of inflammation. We found that aged livers and intestines of iPLA2β$^{-/-}$ mice exhibited altered phospholipid metabolism, increased apoptosis, and inflammation [25]. Consistent with these

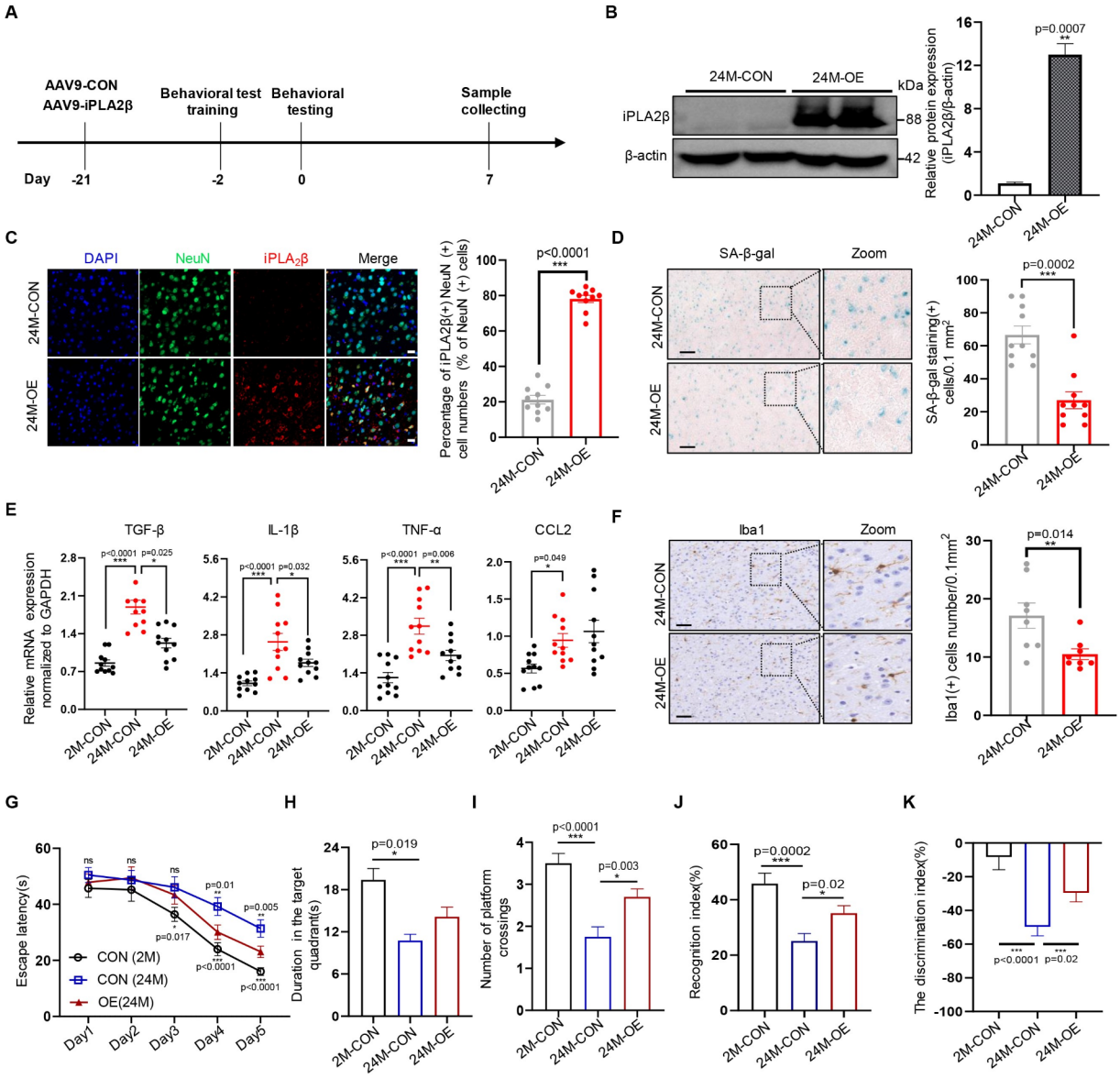

Fig. 8 Overexpression of iPLA2β in PFC improves cognitive function of old mice. **A** Scheme of the experimental design. AAV injections were administered 21 days prior to formal behavioral testing. Behavioral test training sessions were conducted two days before the formal testing began. Samples were collected on the seventh day following the initiation of the formal behavioral experiment. **B** Protein levels of iPLA2β in the 22 M PFC with iPLA2β overexpression (iPLA2β-OE) and control (CON) groups, as assessed by Western blotting and densitometry. **C** Representative immunofluorescence images of iPLA2β (red) and NeuN (green) in the 22 M PFC with iPLA2β overexpression (iPLA2β-OE) and control (CON) groups. Scale bar: 20 μm. **D** Representative SA-β-gal staining images in the 22 M PFC with iPLA2β overexpression (iPLA2β-OE) and control (CON) groups. Scale bar: 100 μm. **E** mRNA expression levels of TGFβ, IL-1β, TNF-α, and CCL2 in the 22 M PFC with iPLA2β overexpression (iPLA2β-OE) and control (CON) groups assessed via qPCR. Normalization was conducted relative to GAPDH expression levels. $n = 11$. **F** Representative IHC images of Iba1 in the 22 M PFC with iPLA2β overexpression (iPLA2β-OE) and control (CON) groups. Histogram showing quantification of the Iba1(+) area. Scale bar: 50 μm. **G** Travel time of the mice to reach the platform during the spatial test. $n = 20$ per group. **H** Duration spent by mice in the hidden platform quadrants during the probe trial. $n = 20$. **I** Frequency of platform crossings by mice during the probe trial. $n = 20$ per group. **J** Recognition index during the Novel object recognition test. Recognition index = time spent exploring a novel object/time spent exploring both objects. $n = 20$. **K** Discrimination index during the Novel object recognition test. The discrimination index = (time spent on the novel object − time spent on the familiar object)/ time spent on both objects. $n = 20$

Data are presented as the mean ± SEM; *p* values were obtained using the Mann-Whitney U test (B, C, D, and F) and the Kruskal-Wallis test followed by Dunn's multiple comparisons test (E, G, H, I, J, and K). * $p < 0.05$. **, $p < 0.01$; ***, $p < 0.001$

findings, the prefrontal cortex (PFC) of aged iPLA2β$^{-/-}$ mice also showed disrupted phospholipid metabolism, elevated apoptosis, and increased levels of pro-inflammatory factors. These changes ultimately lead to cognitive

impairment, underscoring the critical role of iPLA2β in maintaining neuronal health during aging.

Age-associated cognitive impairment has been attributed to various molecular processes, including chronic inflammation, metabolic homeostasis imbalance, and mitochondrial dysfunction. Increased production or decreased clearance of inflammation exacerbates Alzheimer's disease (AD) [50]. Phospholipids in cell membranes act as storage sites for lipid mediator precursors during aging. The levels of inflammatory lipid mediators remain stable until later stages of aging in both AD and wild-type mice, indicating that the expression of certain phospholipid-regulating proteins is age-dependent [51]. Reduced PLA2 activity has been reported in the postmortem brains of patients with AD, and the reduction was correlated with the severity of dementia [52]. However, cPLA2 [53] and sPLA2 [54] have been shown to be upregulated in AD brains, indicating their involvement in inflammatory signaling and the neurodegenerative process. Biallelic loss-of-function variants in iPLA2γ have been associated with mitochondria-related neurodegeneration in patients [55]. In our study, we did not observe significant changes in the mRNA levels of sPLA2, cPLA2, and iPLA2γ in the mouse brain, suggesting that the downregulation of iPLA2β might be one of the reasons for the overall reduction of PLA2 activity in Alzheimer's disease. However, since mRNA and protein expression levels do not correlate in some cases, further research is needed to confirm this. Moreover, by incorporating SA-β-gal staining, we assessed whether the loss of iPLA2β contributes to increased cellular senescence [38].

During brain aging, senescent cells accumulate, and their SASP contributes to age-related inflammation [56]. Reducing senescent neurons has been shown to alleviate the disruptions associated with neurodegenerative diseases in mouse models [57]; however, the impact of iPLA2β deficiency-related senescence on age-related cognitive injury has not been thoroughly investigated. To explore the connection between the accumulation of senescent cells and iPLA2β deficiency, we assessed cellular senescence in the PFCs of iPLA2β knockout and overexpression aged mice. Additionally, we examined the effects of iPLA2β overexpression on neuronal senescence using a D-gal-induced primary neuronal aging model. We demonstrated that iPLA2β reduced neuronal senescence both in vitro and in vivo, which may be due to its role in promoting the clearance of apoptotic cells. iPLA2β has been shown to produce LPC, which serves as a chemotactic "find-me" signal that attracts phagocytes to clear apoptotic cells [58]. Given our observations of reduced LPC levels in aged PFCs with iPLA2β deficiency, it is highly plausible that the regulation of neuronal apoptosis by LPC is a key mechanism contributing to increased susceptibility to aging. Our observation aligns with our previous report demonstrating decreased LPC levels in the gut and liver of aged iPLA2β-deficient mice, resulting in the accumulation of apoptotic cells [27]. In aged PFCs, ineffective clearance of apoptotic cells leads to abnormal neuroinflammation and cellular senescence. These observations suggest a potential link between ineffective apoptotic cell clearance, neuroinflammation, cellular senescence, and cognitive decline in aged brains.

Aging is associated with a decreased capacity to generate ATP in the mitochondria [59]. Here, we found that iPLA2β colocalizes with the mitochondrial membrane protein TOM20 in mPFCs. Given TOM20's role in mitochondrial function and its degradation during mitophagy, the observed decrease in TOM20 levels with iPLA2β overexpression could indicate enhanced mitophagy activity or an adaptive response to mitigate mitochondrial dysfunction. In addition, iPLA2β protects the morphology and ATP production capacity of neuronal mitochondria during aging. This is consistent with the mitochondrial dysfunction observed in GECs lacking iPLA2γ [60]. Mitophagy, which removes damaged mitochondria, is essential for maintaining the quantity and quality of mitochondria. Impairments in mitophagy are associated with abnormal cell differentiation, metabolic dysfunction, and neurodegeneration [61]. Our findings indicate that phospholipid remodeling mediated by iPLA2β is related to mitophagy in neurons. Compared to aged WT PFCs, the mtDNA-to-nuclear DNA ratio in aged iPLA2β knockout PFCs increased significantly by two-fold, indicating an increase in damaged mitochondria. Studies have reported other pathways that increase mtDNA, including TFAM deficiency [62] and the activation of pro-apoptotic proteins [63]. This study found that iPLA2β reduced mitochondrial DNA in aged PFCs by inducing mitophagy. We propose that the deficiency of iPLA2β in aged brains leads to defective mitophagy, resulting in increased release of mtDNA into the cytosol, which in turn increases neuroinflammation and cellular senescence. This links iPLA2β to age-related mitophagy.

Our study elucidated the role of iPLA2β in regulating mitophagy through its influence on phospholipid metabolism. Specifically, iPLA2β appears to enhance mitophagy by modulating the levels of critical phospholipids involved in mitochondrial function. In our experiments, iPLA2β deficiency in the aged prefrontal cortex resulted in notable changes in phospholipid profiles, including decreased levels of lysophosphatidylcholine (LPC) and lysophosphatidylethanolamine (LPE). iPLA2β hydrolyzes polyunsaturated fatty acid-containing phosphatidylcholine (PUFA-PC) and phosphatidylethanolamine (PUFA-PE) to produce LPC 14:0 and LPE 18:0, which are essential for maintaining mitochondrial membrane integrity and function [64, 65]. The mechanistic link between iPLA2β deficiency and neurodegenerative

conditions is evident from the observed impairment of mitophagy. iPLA2β deficiency is associated with downregulation of the mitochondrial fission protein MFF and Parkin-dependent mitophagy proteins, leading to a compromised ability to selectively remove dysfunctional mitochondria [44]. This is consistent with the findings in Parkin-null mice, which showed decreased mitochondrial phosphatidylethanolamine levels and disrupted mitophagy [66]. The reduced LPC and LPE levels observed in our study are similar to the phospholipid disturbances reported in Alzheimer's [67]. Furthermore, disruption of phospholipid metabolism is known to impair mitophagy. For example, yeast cells deficient in autophagy-related protein 32 (Atg32) exhibit defective mitophagy due to altered membrane phospholipid profiles [68]. Our findings suggest that iPLA2β deficiency impairs PINK1- and Parkin-mediated mitophagy pathways by altering phospholipid levels, which are crucial for mitochondrial function. This disruption contributes to the accumulation of dysfunctional mitochondria, which is a hallmark of neurodegenerative diseases. Future research should elucidate the specific pathways and intermediary steps through which iPLA2β modulates mitophagy to better understand its role in neurodegenerative processes.

In this study, we used female mice to investigate iPLA2β's role in aging-related cognitive decline, as female mice often show different neurological responses compared to males, particularly in aging [69]. Factors such as sex hormones and metabolism can lead to sex-specific outcomes [70, 71]. This focus on female mice aims to reduce variability due to sex differences, but this may limit the generalizability of our findings. Future research should include male mice to determine if iPLA2β's effects are consistent across sexes. Additionally, potential confounding factors, such as genetic background and environmental conditions, must be considered. Variations in APOE genotypes [72] and age-related changes, such as inflammation and oxidative stress [73], might affect cognitive outcomes independently of iPLA2β. In addition, the potential side effects or long-term consequences of iPLA2β overexpression should be evaluated. iPLA2β overexpression may disrupt lipid metabolism or cellular processes, leading to unforeseen complications [74]. Thorough preclinical and clinical evaluations are essential to address these issues and ensure the safety and efficacy of iPLA2β-based treatments.

Conclusions

In summary, our findings indicate that a reduction in iPLA2β leads to impaired neuronal mitophagy in the prefrontal cortex, thereby exacerbating age-related cognitive decline. iPLA2β is downregulated in aged PFC, correlating with cognitive function impairment and phospholipid metabolism dysregulation, particularly in the development of LPC and LPE. Enhanced iPLA2β expression alleviated cognitive dysfunction and inflammation in PFCs and increased neuronal mitochondrial function and mitophagy during aging (Fig. 9). This finding provides further support for the development of therapeutic interventions aimed at iPLA2β to enhance phospholipid remodeling, neuronal mitophagy, and cognitive function.

Supplementary Information

The online version contains supplementary material available at https://doi.org/10.1186/s12974-024-03219-z.

Supplementary Material 1

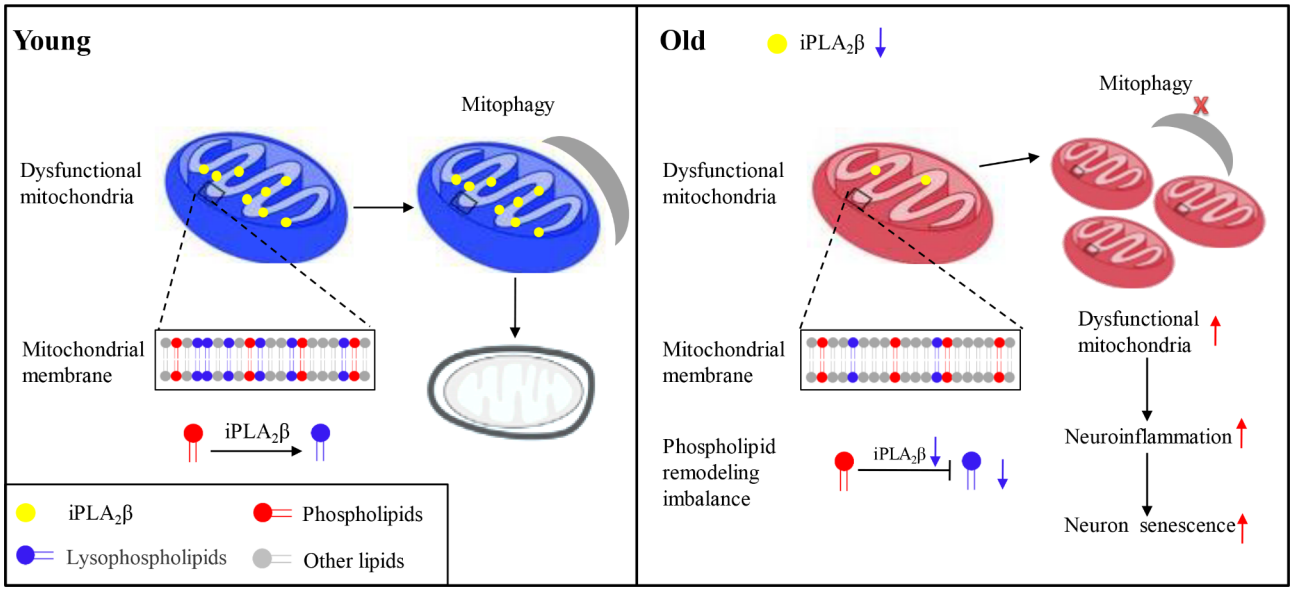

Fig. 9 Possible mechanism underlying the protective effects of iPLA2β on brain aging

Supplementary Material 2

Supplementary Material 3

Supplementary Material 4

Supplementary Material 5

Supplementary Material 6

Supplementary Material 7

Supplementary Material 8

Supplementary Material 9

Supplementary Material 10

Acknowledgements
We acknowledge the assistance of the Xiaozhong Peng group members at the Institute of Basic Medical Sciences, Chinese Academy of Medical Sciences.

Author contributions
Li Jiao was responsible for study design, performing experiments, data analysis, and drafting the manuscript. Wenxin Shao conducted the lipidomic analysis and data analysis. Wenqi Quan and Penghui Liu conducted primary neuron culture. Longjiang Xu assisted with viral injections. Jinling Yang performed the pathological assessments. Xiaozhong Peng was responsible for study design, funding support, manuscript revision, and project supervision. All authors reviewed the manuscript.

Funding
This work was supported by the National Key R&D Program of China (2022YFA1103803), the National Natural Science Foundation of China (82101640), CAMS Innovation Fund for Medical Sciences (2021-I2M-1-024), Non-profit Central Research Institute Fund of the Chinese Academy of Medical Sciences (2019-RC-HL-017), and Peking Union Medical College Central University Basic Research Funding (3332018127).

Data availability
No datasets were generated or analysed during the current study.

Declarations

Ethical approval and consent to participate
All experimental protocols and ethics were approved by the Institutional Ethics Committee of the Chinese Academy of Medical Sciences and Peking Union Medical College.

Consent for publication
All the authors agree with the submission of this manuscript.

Competing interests
The authors declare no competing interests.

Received: 17 June 2024 / Accepted: 1 September 2024
Published online: 18 September 2024

References

1. Lopez-Otin C, et al. Hallmarks of aging: an expanding universe. Cell. 2023;186(2):243–78.
2. Scheltens P, et al. Alzheimer's Disease. Lancet. 2021;397(10284):1577–90.
3. Marchetti B, et al. Parkinson's disease, aging and adult neurogenesis: Wnt/beta-catenin signaling as the key to unlock the mystery of endogenous brain repair. Aging Cell. 2020;19(3):e13101.
4. Hou Y, et al. Ageing as a risk factor for neurodegenerative disease. Nat Rev Neurol. 2019;15(10):565–81.
5. Allen WE, et al. Molecular and spatial signatures of mouse brain aging at single-cell resolution. Cell. 2023;186(1):194–e20818.
6. Mathys H, et al. Single-cell atlas reveals correlates of high cognitive function, dementia, and resilience to Alzheimer's disease pathology. Cell. 2023;186(20):4365–e438527.
7. Rodrigue KM, Raz N. Shrinkage of the entorhinal cortex over five years predicts memory performance in healthy adults. J Neurosci. 2004;24(4):956–63.
8. McEwen BS, Morrison JH. The brain on stress: vulnerability and plasticity of the prefrontal cortex over the life course. Neuron. 2013;79(1):16–29.
9. Rosenberg EC, et al. Cannabidiol modulates excitatory-inhibitory ratio to counter hippocampal hyperactivity. Neuron. 2023;111(8):1282–e13008.
10. Agrawal I, et al. Deciphering lipid dysregulation in ALS: from mechanisms to translational medicine. Transl Neurodegener. 2022;11(1):48.
11. Neniskyte U, et al. Phospholipid scramblase Xkr8 is required for developmental axon pruning via phosphatidylserine exposure. EMBO J. 2023;42(14):e111790.
12. Malley KR, et al. The structure of iPLA(2)beta reveals dimeric active sites and suggests mechanisms of regulation and localization. Nat Commun. 2018;9(1):765.
13. Bao S, et al. Insulin secretory responses and phospholipid composition of pancreatic islets from mice that do not express group VIA phospholipase A2 and effects of metabolic stress on glucose homeostasis. J Biol Chem. 2006;281(30):20958–73.
14. Bakhit Y, et al. PLA2G6-associated late-onset parkinsonism in a Sudanese family. Ann Clin Transl Neurol. 2023;10(6):983–9.
15. Tan J, et al. Analysis of PLA2G6 gene variant in a family affected with infantile neuroaxonal dystrophy. Zhonghua Yi Xue Yi Chuan Xue Za Zhi. 2020;37(1):21–4.
16. Deng X, et al. The role of the PLA2G6 gene in neurodegenerative diseases. Ageing Res Rev. 2023;89:101957.
17. Malik I, et al. Disrupted membrane homeostasis and accumulation of ubiquitinated proteins in a mouse model of infantile neuroaxonal dystrophy caused by PLA2G6 mutations. Am J Pathol. 2008;172(2):406–16.
18. Cheon Y, et al. Disturbed brain phospholipid and docosahexaenoic acid metabolism in calcium-independent phospholipase A(2)-VIA (iPLA(2)beta)-knockout mice. Biochim Biophys Acta. 2012;1821(9):1278–86.
19. Lin G, et al. Phospholipase PLA2G6, a Parkinsonism-associated gene, affects Vps26 and Vps35, retromer function, and ceramide levels, similar to alpha-synuclein gain. Cell Metab. 2018;28(4):605–e6186.
20. Errea O, et al. The disruption of mitochondrial axonal transport is an early event in neuroinflammation. J Neuroinflammation. 2015;12:152.
21. Kinghorn KJ, et al. Loss of PLA2G6 leads to elevated mitochondrial lipid peroxidation and mitochondrial dysfunction. Brain. 2015;138(Pt 7):1801–16.
22. Beck G, et al. Neuroaxonal dystrophy in calcium-independent phospholipase A2beta deficiency results from insufficient remodeling and degeneration of mitochondrial and presynaptic membranes. J Neurosci. 2011;31(31):11411–20.
23. Zhang L, Dai L, Li D. Mitophagy in neurological disorders. J Neuroinflammation. 2021;18(1):297.
24. Zhao Y, et al. ATAD3A oligomerization causes neurodegeneration by coupling mitochondrial fragmentation and bioenergetics defects. Nat Commun. 2019;10(1):1371.
25. Li J, et al. Lysocardiolipin acyltransferase 1 (ALCAT1) controls mitochondrial DNA fidelity and biogenesis through modulation of MFN2 expression. Proc Natl Acad Sci U S A. 2012;109(18):6975–80.
26. Chu CT, et al. Cardiolipin externalization to the outer mitochondrial membrane acts as an elimination signal for mitophagy in neuronal cells. Nat Cell Biol. 2013;15(10):1197–205.
27. Jiao L, et al. Ageing sensitized by iPLA(2)beta deficiency induces liver fibrosis and intestinal atrophy involving suppression of homeostatic genes and alteration of intestinal lipids and bile acids. Biochim Biophys Acta Mol Cell Biol Lipids. 2017;1862(12):1520–33.
28. Raihan O, et al. SFRS11 loss leads to aging-associated cognitive decline by modulating LRP8 and ApoE. Cell Rep. 2020;31(11):107713.
29. Liu Q, et al. Lipoprotein receptor LRP1 regulates leptin signaling and energy homeostasis in the adult central nervous system. PLoS Biol. 2011;9(1):e1000575.
30. Velazquez R, et al. Lifelong choline supplementation ameliorates Alzheimer's disease pathology and associated cognitive deficits by attenuating microglia activation. Aging Cell. 2019;18(6):e13037.
31. Takagi T, et al. De novo inbred heterozygous Zeb2/Sip1 mutant mice uniquely generated by germ-line conditional knockout exhibit craniofacial, callosal and behavioral defects associated with Mowat-Wilson syndrome. Hum Mol Genet. 2015;24(22):6390–402.

32. Hu JJ, et al. Emergence of consciousness from anesthesia through ubiquitin degradation of KCC2 in the ventral posteromedial nucleus of the thalamus. Nat Neurosci. 2023;26(5):751–64.
33. Mann PC. *International harmonization of nomenclature and diagnostic criteria for lesions in rats and mice (INHAND)*. 2019.
34. Yu G, et al. Astrocyte reactivation in medial prefrontal cortex contributes to obesity-promoted depressive-like behaviors. J Neuroinflammation. 2022;19(1):166.
35. Dunn WB, et al. Procedures for large-scale metabolic profiling of serum and plasma using gas chromatography and liquid chromatography coupled to mass spectrometry. Nat Protoc. 2011;6(7):1060–83.
36. Phasuk S, et al. Lack of the peroxiredoxin 6 gene causes impaired spatial memory and abnormal synaptic plasticity. Mol Brain. 2021;14(1):72.
37. Walf AA, Frye CA. The use of the elevated plus maze as an assay of anxiety-related behavior in rodents. Nat Protoc. 2007;2(2):322–8.
38. Debacq-Chainiaux F, et al. Protocols to detect senescence-associated beta-galactosidase (SA-betagal) activity, a biomarker of senescent cells in culture and in vivo. Nat Protoc. 2009;4(12):1798–806.
39. Colangelo AM, Alberghina L, Papa M. Astrogliosis as a therapeutic target for neurodegenerative diseases. Neurosci Lett. 2014;565:59–64.
40. Javanmehr N, et al. Microglia dynamics in aging-related neurobehavioral and neuroinflammatory diseases. J Neuroinflammation. 2022;19(1):273.
41. Chou SM, et al. Neuronal senescence in the aged brain. Aging Dis. 2023;14(5):1618–32.
42. Kumar A, Dogra S, Prakash A. Effect of carvedilol on behavioral, mitochondrial dysfunction, and oxidative damage against D-galactose induced senescence in mice. Naunyn Schmiedebergs Arch Pharmacol. 2009;380(5):431–41.
43. Kobro-Flatmoen A, et al. Re-emphasizing early Alzheimer's disease pathology starting in select entorhinal neurons, with a special focus on mitophagy. Ageing Res Rev. 2021;67:101307.
44. Rana A, et al. Promoting Drp1-mediated mitochondrial fission in midlife prolongs healthy lifespan of Drosophila melanogaster. Nat Commun. 2017;8(1):448.
45. Rappe A, McWilliams TG. Mitophagy in the aging nervous system. Front Cell Dev Biol. 2022;10:978142.
46. Palikaras K, Lionaki E, Tavernarakis N. Mechanisms of mitophagy in cellular homeostasis, physiology and pathology. Nat Cell Biol. 2018;20(9):1013–22.
47. Mauthe M, et al. Chloroquine inhibits autophagic flux by decreasing autophagosome-lysosome fusion. Autophagy. 2018;14(8):1435–55.
48. Forester BP, et al. Age-related changes in brain energetics and phospholipid metabolism. NMR Biomed. 2010;23(3):242–50.
49. Yang C, et al. Rewiring neuronal glycerolipid metabolism determines the extent of Axon Regeneration. Neuron. 2020;105(2):276–92 e5.
50. Gulen MF, et al. cGAS-STING drives ageing-related inflammation and neurodegeneration. Nature. 2023;620(7973):374–80.
51. Emre C, et al. Age-related changes in brain phospholipids and bioactive lipids in the APP knock-in mouse model of Alzheimer's disease. Acta Neuropathol Commun. 2021;9(1):116.
52. Ross BM, et al. Phospholipid-metabolizing enzymes in Alzheimer's disease: increased lysophospholipid acyltransferase activity and decreased phospholipase A2 activity. J Neurochem. 1998;70(2):786–93.
53. Wang S, et al. Calcium-dependent cytosolic phospholipase A(2) activation is implicated in neuroinflammation and oxidative stress associated with ApoE4. Mol Neurodegener. 2022;17(1):42.
54. Yagami T, Yamamoto Y, Koma H. The role of secretory phospholipase A(2) in the central nervous system and neurological diseases. Mol Neurobiol. 2014;49(2):863–76.
55. Shukla A, et al. A neurodegenerative mitochondrial disease phenotype due to biallelic loss-of-function variants in PNPLA8 encoding calcium-independent phospholipase A2gamma. Am J Med Genet A. 2018;176(5):1232–7.
56. Sahu MR, et al. Cellular senescence in the aging brain: a promising target for neurodegenerative diseases. Mech Ageing Dev. 2022;204:111675.
57. Herdy JR, et al. Increased post-mitotic senescence in aged human neurons is a pathological feature of Alzheimer's disease. Cell Stem Cell. 2022;29(12):1637–e16526.
58. Lauber K, et al. Apoptotic cells induce migration of phagocytes via caspase-3-mediated release of a lipid attraction signal. Cell. 2003;113(6):717–30.
59. Navarro A, Boveris A. Rat brain and liver mitochondria develop oxidative stress and lose enzymatic activities on aging. Am J Physiol Regul Integr Comp Physiol. 2004;287(5):R1244–9.
60. Elimam H, et al. Genetic ablation of calcium-independent phospholipase A(2) gamma exacerbates glomerular injury in adriamycin nephrosis in mice. Sci Rep. 2019;9(1):16229.
61. Fang EF, et al. Mitophagy inhibits amyloid-beta and tau pathology and reverses cognitive deficits in models of Alzheimer's disease. Nat Neurosci. 2019;22(3):401–12.
62. West AP, et al. Mitochondrial DNA stress primes the antiviral innate immune response. Nature. 2015;520(7548):553–7.
63. McArthur K et al. BAK/BAX macropores facilitate mitochondrial herniation and mtDNA efflux during apoptosis. Science. 2018;359(6378).
64. Gil-de-Gomez L, et al. Cytosolic group IVA and calcium-independent group VIA phospholipase A2s act on distinct phospholipid pools in zymosan-stimulated mouse peritoneal macrophages. J Immunol. 2014;192(2):752–62.
65. Murakami M, et al. Group VIB Ca2+-independent phospholipase A2gamma promotes cellular membrane hydrolysis and prostaglandin production in a manner distinct from other intracellular phospholipases A2. J Biol Chem. 2005;280(14):14028–41.
66. Gaudioso A, et al. Lipidomic alterations in the mitochondria of aged parkin null mice relevant to autophagy. Front Neurosci. 2019;13:329.
67. Fernandes T et al. Mapping the lipidome in mitochondria-associated membranes (MAMs) in an in vitro model of Alzheimer's disease. J Neurochem. 2024.
68. Sakakibara K, et al. Phospholipid methylation controls Atg32-mediated mitophagy and Atg8 recycling. EMBO J. 2015;34(21):2703–19.
69. Li R, Singh M. Sex differences in cognitive impairment and Alzheimer's disease. Front Neuroendocrinol. 2014;35(3):385–403.
70. Eissman JM, et al. Sex differences in the genetic architecture of cognitive resilience to Alzheimer's disease. Brain. 2022;145(7):2541–54.
71. Acaz-Fonseca E, et al. Sex differences and gonadal hormone regulation of brain cardiolipin, a key mitochondrial phospholipid. J Neuroendocrinol. 2020;32(1):e12774.
72. Belloy ME, et al. APOE genotype and Alzheimer disease risk across age, sex, and population ancestry. JAMA Neurol. 2023;80(12):1284–94.
73. Sharma V, Mehdi MM. Oxidative stress, inflammation and hormesis: the role of dietary and lifestyle modifications on aging. Neurochem Int. 2023;164:105490.
74. Yu J, Li T, Zhu J. Gene therapy strategies targeting aging-related diseases. Aging Dis. 2023;14(2):398–417.

Publisher's note